

# Analysis of Scales Formed During Air Oxidation of Co-Ta Alloys at 800°C

M. Castro-Rebello<sup>1</sup>; I.J. Sayeg<sup>2</sup>; J.A.S. Tenório<sup>1</sup> and S. Wolyneć<sup>1</sup>

<sup>1</sup>Departamento de Engenharia Metalúrgica e de Materiais / Escola Politécnica da Universidade de São Paulo - USP / Av. Prof. Mello Moraes, 2463 / CEP 05508-900 / São Paulo - SP / BRASIL

☎ 55 11 3091.5240, Fax 3091.5421, E-mail: marc@usp.br <sup>2</sup>Instituto de Geociências / USP

## Abstract

The air oxidation of three Co-Ta alloys containing 15, 30 and 45 wt.%Ta was investigated with a thermobalance at 800°C. The oxidation morphologies and compounds were analyzed by scanning electron microscopy, energy dispersive X-ray spectrometry and x-ray diffraction. For the first two compositions the oxidation kinetics follows the parabolic rate law while the Co-45Ta alloy presents a behavior intermediate between linear and parabolic. The oxidation morphologies of Co-15Ta and Co-30Ta alloys are very similar. They display an external Co<sub>3</sub>O<sub>4</sub>/CoO duplex scale, and an internal heterophasic region (HR), in which both metallic phases were oxidized. The Co-45Ta alloy displays an external monolayer of Co<sub>3</sub>O<sub>4</sub>, and an internal oxidation zone (IOZ), where only the Ta-rich phase was oxidized.

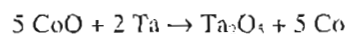
**Keywords:** high-temperature oxidation, Co-Ta alloys, refractory metals, thermogravimetry

## Introduction

Refractory metals bearing alloys have been considered as candidate materials for high-temperature sulfur containing atmospheres. Alloys containing Mo and Nb have been tested for this purpose (6,8). Alloys containing Ta, in particular Co-Ta alloys, also have been considered for this application, but so far only their resistance in oxygen bearing atmospheres has been evaluated (2,4).

The oxidation of binary Co-Ta alloys (10 and 15 wt.%Ta) as well as of the same alloys containing carbon (up to 1 wt.%C) was investigated by El-Dahshan and Hazzaa (4) in pure oxygen and in air, at temperatures ranging from 900°C to 1,100°C. They found that Ta additions reduce the oxidation rate of Co more efficiently than Cr additions. The oxidized alloys exhibit an external monolayer of CoO and a multi-phase porous internal layer composed of CoO, Ta<sub>2</sub>O<sub>5</sub> and CoTaO<sub>4</sub>. The beneficial effect of Ta was attributed to the formation of CoTaO<sub>4</sub>, which would be responsible for the reduction of oxygen activity at metal/oxide interface, blocking its inward diffusion.

Voitovich (9) investigated similar alloys and concluded that the positive effect of Ta is due to the removal of CoO (which presents high concentration of cationic defects) from the external layer through the following redox reaction:



The present investigation is part of a broader study of high-temperature oxidation resistance of refractory metals bearing alloys in different oxygen and sulfur containing atmospheres (2). Its aim is to obtain further information on Co-Ta alloys behavior in high-temperature air atmosphere so as to better understand the oxidation mechanism of these two-phase materials.

## Materials and Methods

Three Co-Ta alloys, containing about 15, 30 and 45 wt.%Ta (Co-15Ta, Co-30Ta and Co-45Ta, respectively), were prepared by repeatedly arc-melting appropriate amounts of the two pure metals (99.5%Co and 99.8%Ta) on a water-cooled copper hearth under high-purity Ti-gettered argon. After cooling, the alloys were annealed under argon atmosphere at 900°C for 48 hours.

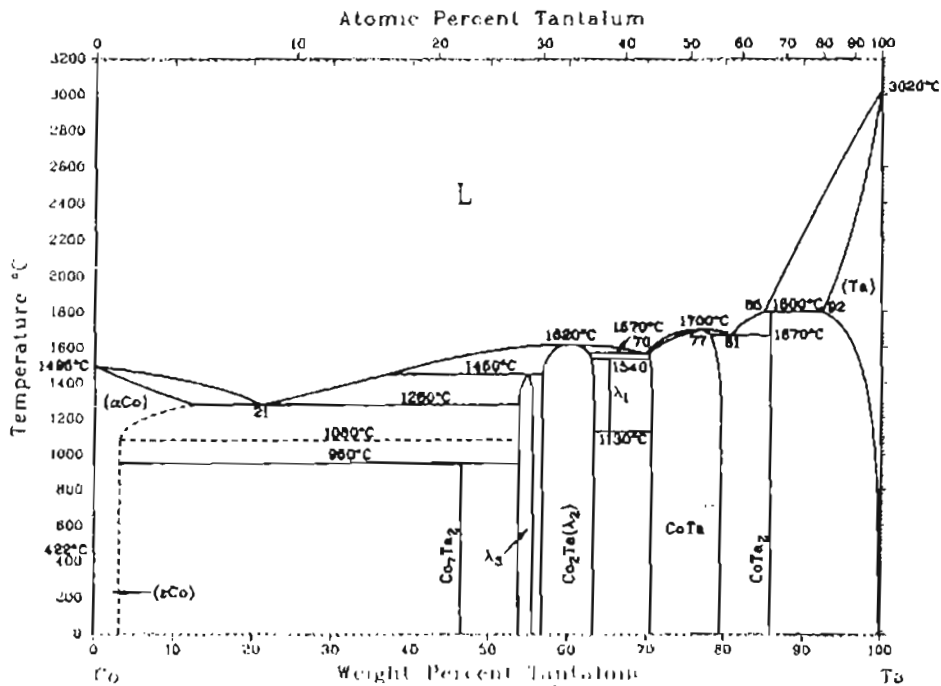


Figure 1 - Co-Ta equilibrium phase diagram (1).

The microstructure of the three alloys is always formed by a cobalt rich phase with maximum Ta content equivalent to 3 wt.% ( $\epsilon$ Co) and the intermetallic phase  $\text{Co}_7\text{Ta}_3$  ( $\lambda_2$ ) (3). This microstructure does not agree with the phase diagram for Co-Ta system, shown in Figure 1 (1), which predicts the formation of a peritectoid phase. This peritectoid phase,  $\text{Co}_7\text{Ta}_3$ , has not been detected by either XRD or EDS. The absence of this phase is probably a consequence of the slow kinetics of the peritectoid reaction, which normally needs controlled cooling or special long-term heat treatments to allow the formation of its product.

Samples of about 1.0 mm thick and with a surface area of approximately 2.0  $\text{cm}^2$  were cut from the ingots using a diamond-wheel saw. They were ground down to 600-grit paper, cleaned with ethanol, ultrasonically rinsed in acetone and dried immediately before use.

The isothermal oxidation tests were carried out at 800°C for periods of 18 hours, in a SHIMADZU TGA-51H thermobalance with continuous weight-gain measurements. Oxidized samples were examined by X-ray diffraction (XRD) for phase identification (PHILIPS PW1710, Cu-K $\alpha$ , spinning). Subsequently, they were mounted in epoxy resin for examination of their transversal sections at scanning electron microscope (SEM) and microanalysis with the energy dispersive X-ray spectrometer (EDS) attachment to the SEM, in order to identify the phases and to determine the element distribution in oxide scales. The SEM used was a PHILIPS XL 30, having a tungsten filament, operating

with an accelerating voltage of 20 kV, in the BSE mode and a working distance varying from 7 to 11 mm.

## Results

All samples, except the Co-45Ta alloy, oxidize according to the parabolic rate law, as shown in Figures 2 and 3. Figure 4 is the di-log plot of the kinetics presented by the tantalum richest alloy which indicates a behavior intermediate between linear and parabolic (slope of approximately 0.8).

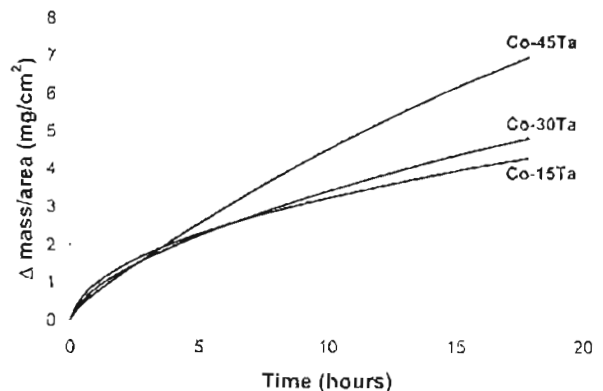


Figure 2 - Kinetics curves for the air oxidation at 800°C of Co-15Ta, Co-30Ta and Co-45Ta.

The oxidation of Co-15Ta and Co-30Ta alloys produced very similar morphologies (figures 5 and 6, respectively). In both alloys external and internal scales were formed. The external is a duplex scale type with  $\text{Co}_3\text{O}_4$  being the outermost and  $\text{CoO}$  the innermost layer. The approximate ratio between the thickness of the  $\text{Co}_3\text{O}_4$  layer and that of  $\text{CoO}$  is 1:3 for Co-15Ta and 1:4 for Co-30Ta.

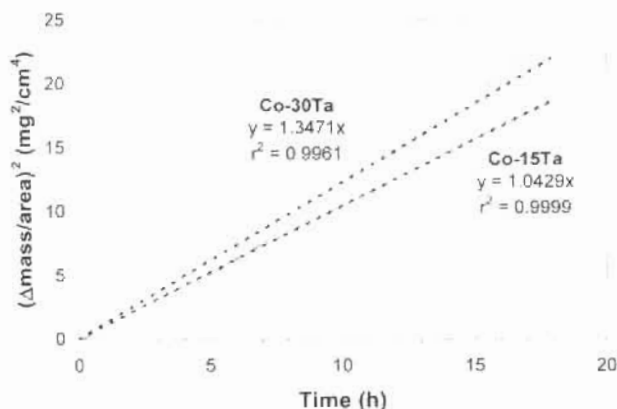


Figure 3 – Parabolic plots of the kinetics curves for the air oxidation at 800°C of Co-15Ta and Co-30Ta. The values of corresponding parabolic rate constants,  $k_p$  ( $y = k_p x$ ), and of the r-squared correlation coefficient,  $r^2$ , of the fitted straight lines are also shown.

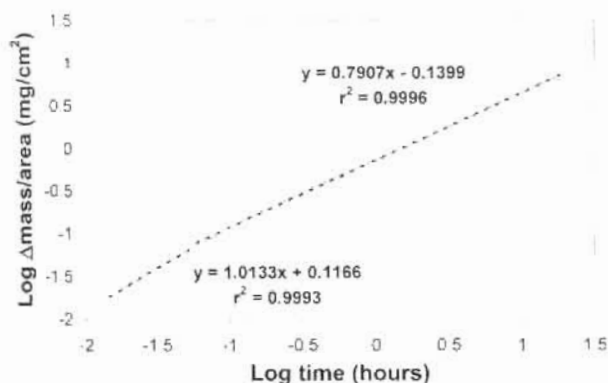


Figure 4 – Di-log plot of the kinetics curve for the air oxidation at 800°C of Co-45Ta (first part – up to 3 minutes, second part – from 3 minutes to 18 hours). The corresponding equations of the fitted straight lines and the respective r-squared correlation coefficient,  $r^2$ , are also shown.

The internal scale has a two-phase microstructure, resembling that of the alloys, i.e., the spatial distribution of the oxide phases is exactly the same as that of the metallic phases present in the alloys before their oxidation. The EDS analysis confirmed that both metallic phases become oxidized. This type of distribution is known as heterophasic region (HR). The thickness of this region is equal to 23  $\mu\text{m}$  and 26  $\mu\text{m}$ , respectively, for Co-

15Ta and Co-30Ta alloys. Figure 7 shows in detail the HR-alloy interface at the Co-15Ta alloy, where it can be verified the good adherence along this interface.

The Co-45Ta alloy displayed an external monolayer of  $\text{Co}_3\text{O}_4$  and a thick region of internal attack (57  $\mu\text{m}$ ) (Figure 8). The morphology of this region is different from that observed on Co-15Ta and Co-30Ta alloys, since only the intermetallic phase was oxidized. This suggests that an internal oxidation zone (IOZ) was formed. However, in a similar way to the more diluted alloys, the internal scale of Co-45Ta alloy shows no spatial distribution difference when compared to that of metallic alloy. Actually, it is believed that Ta was oxidized in both metallic phases, although this oxidation is only visible in the intermetallic phase, due to contrast reasons.

The XRD analysis of oxidized Co-15Ta alloy detected, besides the superficial formed  $\text{Co}_3\text{O}_4$  and  $\text{CoO}$ , also the double oxides  $\text{CoTa}_2\text{O}_6$  and  $\text{Co}_4\text{Ta}_2\text{O}_9$ . These double oxides were not detected at the oxidized Co-30Ta alloy, although the EDS analysis of this alloy indicated a possible presence of this type of oxides. These contradictory results may indicate that, instead of double oxides, tantalum-rich phase could have formed a mixture of  $\text{Ta}_2\text{O}_5$  plus either  $\text{CoO}$  or metallic  $\text{Co}$ , which lead EDS microanalysis to a chemical composition close to that of the double oxides.

The XRD analysis of oxidized Co-45Ta detected some nitrogen-containing phases: tantalum nitrides ( $\text{Ta}_2\text{N}$ ,  $\text{Ta}_3\text{N}$  and  $\text{Ta}_4\text{N}$ ) and  $\text{Co}(\text{NO}_3)_2$ . These phases were not identified in the scales because the EDS microprobe was used to analyze only Co, Ta and O.

## Discussion

As was already stated, there is a significant difference between the oxidized scale morphology of Co-15Ta and Co-30Ta alloys and that of Co-45Ta alloy. The main difference is the type of internal scale, since in the latter an internal oxidation zone (IOZ) was formed, in which only the Ta-rich phase was oxidized, while for the two first alloys a heterophasic region (HR) was formed, in which both metallic elements were oxidized.

When no metallic diffusion occurs and only one alloy element is oxidized by the inward diffusion of oxygen this type of internal oxidation of two-phase alloys is called "diffusionless" or "in situ" internal oxidation (5). The inward oxygen diffusion causes a progressive drop of oxygen partial pressure. At a certain depth, the oxygen partial pressure is not sufficient to oxidize Co but can still oxidize Ta, since the latter is more reactive (less noble) than Co. Therefore, the internal scale that was detected on Co-15Ta and Co-30Ta alloys, where both metallic phases (and both metallic elements, as well) were oxidized, cannot be considered as due to internal oxidation. This implies that the oxygen partial pressure at the reaction front is higher than the dissociation pressure of  $\text{CoO}$ .

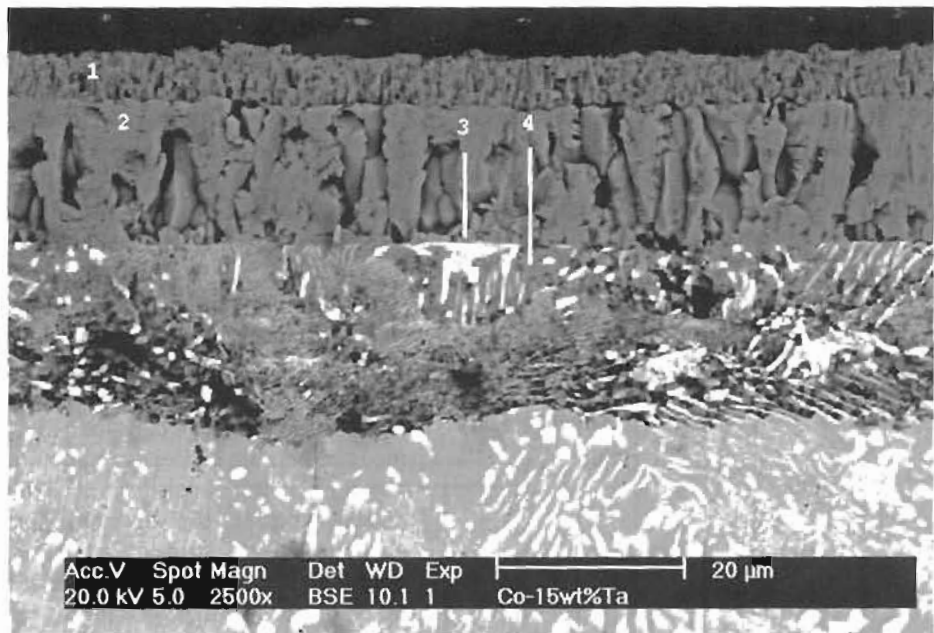


Figure 5 – Cross section of Co-15Ta alloy oxidized in air at 800°C for 18 hours (BSE/2500×). 1 and 2: external duplex scale (1 -  $\text{Co}_3\text{O}_4$  and 2 -  $\text{CoO}$ ); 3 and 4: heterophasic region - HR (3 – oxidized Ta-rich phase and 4 – oxidized Co rich phase).

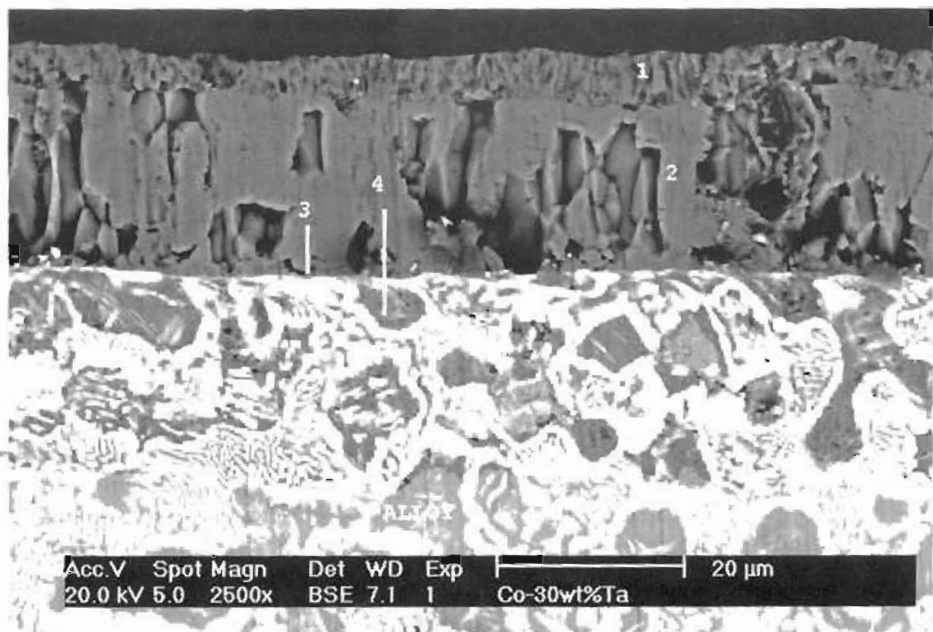


Figure 6 – Cross section of Co-30Ta alloy oxidized in air at 800°C for 18 hours (BSE/2500×). 1 and 2: external duplex scale (1 -  $\text{Co}_3\text{O}_4$  and 2 -  $\text{CoO}$ ); 3 and 4: heterophasic region - HR (3 – oxidized Ta-rich phase and 4 – oxidized Co rich phase).

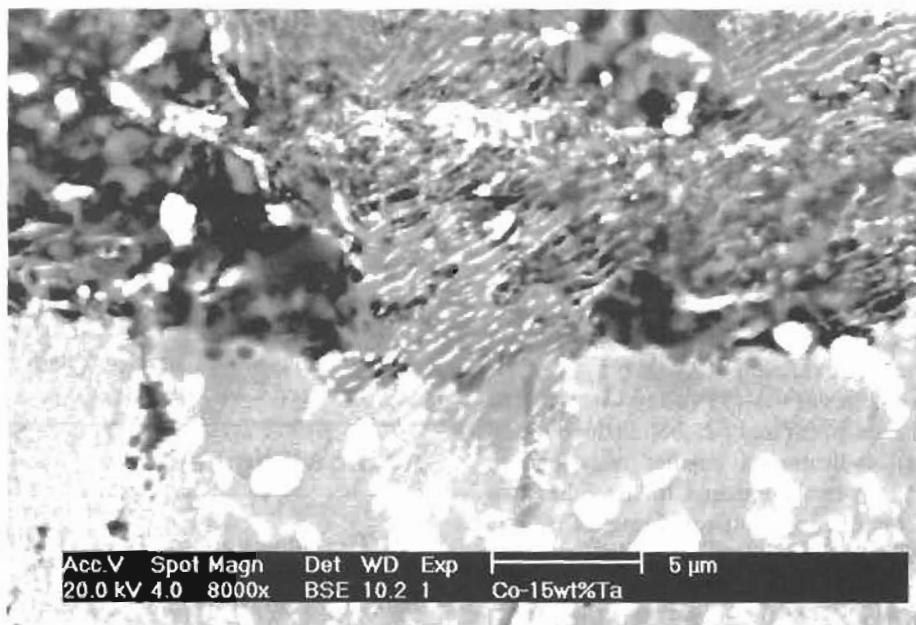


Figure 7 – Detail of the interface between the alloy and the heterophasic region on Co-15Ta alloy, oxidized in air at 800°C for 18 hours (BSE/8000 $\times$ ). Top: heterophasic region; bottom: non-oxidized alloy.

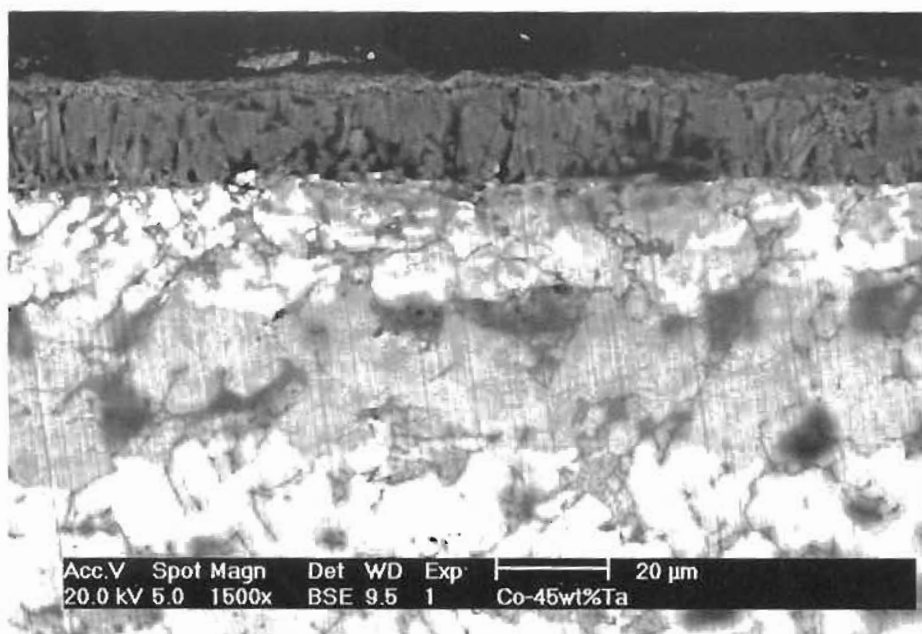


Figure 8 – Cross section of Co-45Ta alloy oxidized in air at 800°C for 18 hours (BSE/1500 $\times$ ). Top: external monolayer of  $\text{Co}_3\text{O}_4$ , intermediate: internal oxidized zone (IOZ), bottom: non-oxidized alloy.

This type of internal attack (HR) may also coexist with another more internally located scale, in which only the more reactive metal is oxidized, giving rise to an IOZ. This IOZ is characterized by a morphology in which only the phase that contains the most reactive element is oxidized such as the one observed in Co-45Ta alloy. Nevertheless, the presence of this IOZ beneath the HR was not observed in either Co-15Ta or Co-30Ta alloys. The absence of IOZ's in these alloys suggests a possible

obstruction of oxygen diffusion through the HR. This obstruction is certainly related to the nature of the oxidation products of this layer.

Another factor, which could have contributed to the different type of internal oxidation at Co-45Ta alloy, is the volume fraction of Ta-rich phase ( $\lambda_3$ ), which is approximately 90%. Even if oxygen partial pressure is sufficient to oxidize Co, the much bigger  $\lambda_3$ -volume fraction determines a greater possibility for oxygen to

meet Ta rather than Co. Moreover, there is also the kinetics factor. If the growing rate of Ta oxides is greater than that of Co oxides (what is normally observed at conditions of high oxygen pressure), then Ta oxides may grow and coalesce, isolating Co-rich phase from oxygen attack. For this mechanism to be operative there is a demand of a minimum volume fraction of  $\lambda_3$ , i.e., there must be a critical volume fraction of Ta-rich phase to suppress the oxidation of Co. This critical  $\lambda_3$ -volume fraction seems to be between that found in Co-30Ta alloy (which formed HR) and that of Co-45Ta alloy (which formed IOZ with the sole oxidation of  $\lambda_3$ ).

The oxidation kinetics of Co-45Ta alloy was found to be intermediate between linear and parabolic (slope of 0.8 on the di-log plot), indicating a smaller resistance to oxidation of Co-45Ta when compared to the other two alloys. Apparently, the oxygen diffusion through  $\text{Co}_3\text{O}_4$  is much easier than through CoO.

The literature data (7) state that the oxygen diffusion coefficient in  $\text{Co}_3\text{O}_4$  is  $2.4 \times 10^{-22} \exp[-736(\text{kJ/mol})/RT]$   $\text{m}^2/\text{s}$  while in CoO it is  $8.8 \times 10^{-21} \exp[-287(\text{kJ/mol})/RT]$   $\text{m}^2/\text{s}$ . The data for CoO was determined in the range of 1,050°C to 1,300°C, while for  $\text{Co}_3\text{O}_4$  there is no information as to the temperature range in which it is valid. However, if it is assumed that these values are valid at 800°C, then the oxygen diffusion coefficients for  $\text{Co}_3\text{O}_4$  and CoO would be  $3.41 \times 10^{-14} \text{ m}^2/\text{s}$  and  $9.24 \times 10^{-18} \text{ m}^2/\text{s}$ , respectively. This is in agreement with the above finding.

According to Figure 3, Co-15Ta is more resistant to oxidation compared to Co-30Ta. So in the present Co-Ta system, the higher the Ta content of the alloy the faster is its oxidation.

Further diffusion and thermodynamic data related to Co-Ta-O and Co-Ta-N systems, in particular diffusion paths in ternary diagrams, would allow a better understanding of alloys' oxidation. This complementary study will be presented elsewhere.

## Conclusions

- The air oxidation kinetics at 800°C of Co-15Ta and Co-30Ta alloys is parabolic (Co-30Ta has a  $k_p$  higher than that of Co-15Ta), while that of Co-45Ta alloy is intermediate between linear and parabolic (the di-log kinetics curve displays a slope of 0.8).
- The oxidation of Co-15Ta and Co-30Ta produced an external duplex scale, formed by  $\text{Co}_3\text{O}_4$  and CoO, and an internal heterophasic region (HR), in which both metallic phases were oxidized and their spatial distribution is exactly the same as that of the metallic phases present in the alloys before oxidation.
- The oxidation of Co-45Ta alloy produced an external  $\text{Co}_3\text{O}_4$  monolayer, and an internal oxidation zone

(IOZ), in which only the Ta-rich phase suffered oxidation.

- The IOZ formed at the Co-45Ta alloy is much thicker than the HR's presented by the two other alloys, which appears to be a consequence of the nature of its external monolayer and also of the exclusive internal oxidation of Ta (determining a lesser consumption of oxygen per unit of volume).
- To better understand the Co-Ta alloys air oxidation it will be necessary to take into account the nitrogen compounds which were detected by XRD in the scale of oxidized Co-45Ta alloy.

## Acknowledgments

The authors are grateful to FAPESP for the funding of the present research project (Processes: 95/0086-2, 98/9570-2 and 01/06056-0). One of us (MCR) expresses his gratitude for his PhD and Pos-Doc scholarships (94/2249-3 and 98/15742-0, respectively), granted by FAPESP.

## References

1. Baker, H., ed. (1992) Alloy Phase Diagrams.. ASM International, Materials Park, Ohio, v. 3, p. 149.
2. Castro-Rebello, M. (1999) High temperature oxidation of niobium or tantalum bearing experimental alloys. Doctor Thesis. Escola Politécnica da Universidade de São Paulo, São Paulo, 222 p (in Portuguese).
3. Castro-Rebello, M., Bianchi, F.F., Sandim, H.R.Z., Tenório, J.A.S. and Wolynec, S. (2001) Metalurgia e Materiais (Caderno Tecnológico ABM: Engenharia e Aplicação de Materiais nº 1) 57(516):3-8 (in Portuguese).
4. El-Dahshan, M.E. and Hazzaa, M.I. (1987) Werkst. u. Korros. 38:422-431
5. Gesmundo, F., Niu, Y. and Viani, F. (1995) Oxid. Met. 43:379-394
6. Kai, W., Douglass, D.L. and Gesmundo, F. (1992) Oxid. Met. 37:189-198
7. Kofstad, P. (1988) High Temperature Corrosion. Elsevier Applied Science, London & New York, pp. 99-100.
8. Mrowec, S. and Przybylski, K. (1985) Oxid. Met. 23:107-117
9. Voitovich, R.F. (1966) *apud op. cit.* (4) p.424.